

Earthquake sequencing: Analysis of time-series constructed from the Markov chain model

M. S. Cavers¹ and K. Vasudevan^{1,2}

¹Department of Mathematics and Statistics
University of Calgary, Calgary, AB T2N 1N4, Canada
mcavers@ucalgary.ca, vasudeva@ucalgary.ca

²Department of Geoscience
University of Calgary, Calgary, AB T2N 1N4, Canada
vasudeva@ucalgary.ca

Abstract. Directed graph representation of a Markov chain model to study global

2 earthquake sequencing leads to a time-series of state-to-state transition

probabilities that includes the spatio-temporally linked recurrent events in the

4 record-breaking sense. A state refers to a configuration comprised of zones with

either the occurrence or non-occurrence of an earthquake in each zone in a pre-

6 determined time interval. Since the time-series is derived from non-linear and

non-stationary earthquake sequencing, we use known analysis methods to glean

8 new information. We apply decomposition procedures such as ensemble empirical

mode decomposition (EEMD) to study the state-to-state fluctuations in each of the

10 intrinsic mode functions. We subject the intrinsic mode functions, derived from

the time-series using the EEMD, to a detailed analysis to draw information-content

12 of the time-series. Also, we investigate the influence of random-noise on the data-

driven state-to-state transition probabilities. We consider a second aspect of

14 earthquake sequencing that is closely tied to its time-correlative behavior. Here,

we extend the Fano factor and Allan factor analysis to the time-series of state-to

16 state transition frequencies of a Markov chain. Our results support not only the

usefulness the intrinsic mode functions in understanding the time-series but also

18 the presence of power-law behaviour exemplified by the Fano factor and the Allan

factor.

20

1 Introduction

2 Earthquake sequencing has been the subject of detailed research (Nava et al., 2005;
Ünal and Çelebioğlu, 2011, 2014; Telesca et al., 2001, 2008, 2009, 2011; Cavers
4 and Vasudevan, 2013, 2015; Vasudevan and Cavers, 2012, 2013) both in the
regional and global sense in recent years. Nava et al. (2005) have introduced the
6 Markov chain model to study the earthquake sequencing in a seismogenically active
region where the region is partitioned into zones. The functionality of the method
8 is determined by the characteristics of the state-to-state transitions where each state
is described by the earthquake occupancy of the zones. In particular, for a given
10 number of zones, N , a state corresponding to a time interval is expressed as a
concatenation of binary digits $b_{N-1}...b_1b_0$, where $b_L = 1$ (or $b_L = 0$) indicates there
12 was (or was not) an earthquake occurrence in zone L during the specified time
interval. Thus, states can fall into zones of no occupancy to full occupancy at the
14 extreme and into zones where some are occupied and some are not. The approach
of Nava et al. (2005) was immediately extended to other regions (Herrera et al.,
16 2006; Ünal and Çelebioğlu, 2011, 2014). Cavers and Vasudevan (2013) adapted
the method of Nava et al. (2005) to a global catalogue which was partitioned into
18 zones on the basis of the tectonic boundaries (DeMets et al. (1990, 2010), Bird
(2003), Kagan et al., 2010). The existing Markov chain model was refined by
20 incorporating the record-breaking recurring events for each event in the catalogue
under certain constraints. A directed graph representation of the modified Markov
22 chain model was then subjected to detailed analysis for forecasting purposes (Cavers
and Vasudevan, 2015).

24 One consequence of the approach taken by Cavers and Vasudevan (2015) and
Vasudevan and Cavers (2013) is that it results in a time-series of state-to-state

transition frequencies of the modified Markov chain model, $x_{stf}(t)$. This time-series
is for an optimized time-interval, Δt . The fluctuations in state-to-state transitions
are Δt sampled. The time-series is a comprehensive representation of earthquake
sequencing in which interaction of seismic events within and among zones are
considered. Therefore, it can be subjected to a detailed analysis.

Earthquake sequencing may be considered a non-linear and non-stationary
process (Kanamori, 2003; Telesca et al., 2001, 2008, 2009, 2011; Flores-Marquez
and Valverde-Esparza, 2012). In earthquake sequencing, earthquakes are viewed as
part of a point process, with earthquake events occurring at some random locations
in time. This means that the earthquake sequencing is dictated by the set of event
times, and can also be expressed by the set of time-intervals between events. The
time-series of earthquakes for any time-interval can be analyzed in many ways
(Telesca et al., 2001, 2008, 2009, 2011).

We postulate here that the non-linear and non-stationary behavior in the time-
series should also be present in the time-series of the state-to-state transition
frequencies derived from earthquake sequencing. Hence, we consider the
approaches of Telesca et al. (2001, 2008, 2009, 2011) to be appropriate for a study
here.

Non-linear and non-stationary time-series have been examined in recent years
with a method known as empirical mode decomposition (EMD) and the intrinsic
mode functions derived from this are useful in this regard (Huang et al., 1998). The
present time-series of state-to-state transition frequencies is suited for such a study.

In general, the time-series has non-zero amplitudes for the state-to-state
transition frequencies (Cavers and Vasudevan, 2015). In this particular case, there

are instances where there are no earthquakes exceeding the magnitude of 5.6 in all zones for one or more time steps. This introduces “intermittency” in the time series.

However, because of the presence of intermittency in it, an ensemble approach to empirical mode decomposition, EEMD (Wu and Huang, 2004, 2009; Flandrin et al., 2004, 2005) is applied here. The intermittency problem is handled with the addition of random noise to the time-series before carrying out the EEMD (Wu and Huang, 2009). We examine the criteria used for the selection of the added noise and the ensemble number for the EEMD.

Another aspect of the study here is to ask a question if the time-series resulting from a directed graph representation of the Markov chain model of earthquake sequences exhibits power-law statistics similar to a description of fractal stochastic point processes (Telesca et al., 2001, 2009, 2011) to model the time-occurrence-sequence of seismic events. Quantifying the earthquake sequencing in terms of its fractal properties was done by means of the Fano factor and the Allan factor (Allan, 1966; Barnes and Allan, 1966; Lowen and Teich, 1993, 1995; Thurner et al., 1997; Telesca et al., 2001, 2009, 2011; Flores-Marquez and Valverde-Esparza, 2012; Serinaldi and Kilsby, 2013). Since the fractal properties of the time-series studied here has never been investigated, we calculate the Fano factor and the Allan factor for the purpose of quantitative analysis.

The remainder of the paper is divided into three sections. In the next section, we show how the time-series of the state-to-state transition frequencies for a modified Markov chain model as described in Cavers and Vasudevan (2015) is generated. In the following section, we describe the EEMD procedure used and the analysis of the results that accrue from this procedure. We extend the approaches of Telesca et al. (2001, 2008, 2009, 2011) to calculate the Fano factor and the Allan factor with a

view to study the fractal properties of the time-series. In the last section, we discuss the results of the analysis methods and draw certain inferences about the state-to-state transition frequencies.

2 Directed graph representation of earthquake sequencing

A *Markov chain* is a discrete-time stochastic process $X = \{X_0, X_1, X_2, \dots\}$ with state space S where $\Pr\{X_{n+1} = j \mid X_0, \dots, X_n\} = \Pr\{X_{n+1} = j \mid X_n\}$, for all j in S and n in $\{0, 1, 2, \dots\}$. For each n , the state of X_{n+1} is independent of X_0, X_1, \dots, X_{n-1} given X_n , and furthermore, we assume $\Pr\{X_{n+1} = j \mid X_n = i\}$ is independent of n (Çınlar, 1975). To build a Markov chain model we first partition the region, either local or global, into zones. Typically these zones are made up of rectangles that divide the region (Nava et al., 2005; Ünal and Çelebioğlu, 2011). Recently, other partitions have been used. In particular, Cavers and Vasudevan (2015) used a simplified 5-zone plate boundary template as given by Kagan et al. (2010) to study global seismicity, while Ünal et al. (2014) used a seismic zones map that uses geographic information system analysis to divide Turkey into regions. For this particular study, we used the five-zone model described in Cavers and Vasudevan (2015) and give an overview of its construction here.

Kagan et al. (2010) partitioned the shallow (≤ 70 km-depth) events with moment magnitude, $M_w > 5.6$ from the Global CMT catalogue (1982/01/01-2007/03/31) into 5 zone sub-catalogues using their grid-assignment schemes (Table 1). The selected catalogue consists of 6752 earthquakes with 4407 from **Zone 4** (Trenches), 723 from **Zone 3** (Fast-spreading ridges), 487 from **Zone 2** (Slow-spreading ridges), 898 from **Zone 1** (Active continent), and 237 from **Zone 0** (Plate interior) respectively. For these five zones, we express a state, corresponding to a time interval Δt , as a

concatenation of binary digits $b_4b_3b_2b_1b_0$, where $b_L = 1$ indicates an earthquake

2 occurrence in zone L during the specified time interval Δt , and $b_L = 0$ indicates the lack of an earthquake occurrence in zone L during the specified time interval Δt .

4 We use $\Theta = [\theta_{ij}]$ to denote the transition frequency matrix, where θ_{ij} is the number of occurrences of transitions from state i to state j . Letting $s(n)$ represent the state

6 for interval number n , the probability transition matrix, $P = [p_{ij}]$, consists of transition probabilities, p_{ij} , given as

$$8 \quad p_{ij} = \Pr \{s(n+1) = j \mid s(n) = i\} = \Pr \{j|i\}, \quad (1)$$

$$p_{ij} = \theta_{ij} / \zeta_{ij}, \text{ where } \zeta_{ij} = \sum_j \theta_{ij}. \quad (2)$$

10 A finite-state Markov chain can be depicted using a digraph representation, G , where the set of possible states (binary strings of length 5) are the nodes, and an arc

12 (i, j) connects two states i and j if and only if $p_{ij} > 0$ (Jarvis and Shier, 1996). Figure

1 shows an example of a digraph representing a Markov chain with a three zone

14 partition, hence, there there are $2^3 = 8$ states $\{000, 001, 010, 011, 100, 101, 110, 111\}$ that we write in decimal format $\{0, 1, 2, 3, 4, 5, 6, 7\}$, respectively. In this

16 figure, we do not show all of the possible transitions between states and typically an arc (i, j) is omitted when $p_{ij} = 0$. We follow the same decimal state labelling format

18 as in Figure 1 for our $2^5 = 32$ states, that is, state ‘0’ (representing 00000 in binary) corresponds to no earthquake occurrence in all five zones in the chosen time

20 interval, Δt , and state ‘31’ (representing 11111 in binary) points to earthquake occurrences in all five zones. Table 2 shows details for defining all other states, ‘1’

22 to ‘29’.

For a Markov chain structure given earlier for the five zones, the computation

24 of transition frequencies and hence, transition probabilities, depend on the chosen time-interval, Δt . We use the simple rules outlined by Nava et al. (2005) to choose

Δt :

1. Δt should be small enough such that the hazard estimations are useful;
2. Δt should not be too small that the most frequently occurring transition is from state 0 to state 0;
3. Δt should not be too large that state 31 to state 31 transitions are dominant.

So, for the threshold magnitudes chosen, Δt should be large enough to allow interaction among regions and make estimates of Markov chain transition probabilities robust. Following the selection rules given elsewhere (Nava et al., 2005; Ünal and Çelebioğlu, 2011; Cavers and Vasudevan, 2015), we used a Δt value of 9 days for the construction of the Markov chain of transition probabilities. The combinatorial structure of a digraph representation of the Markov chain model contains important information for earthquake sequencing (Cavers and Vasudevan, 2015). It is often useful to use a weight, w_{ij} , for each arc (i, j) of the digraph to get a weighted digraph. The weights have the form $w_{ij} = \theta_{ij}$, $w_{ij} = p_{ij}$, or can be empirically derived from the Markov chain. To introduce spatial-temporal complexity into the model so that transitions with earthquake occurrences at large distances have less of an impact on our model than transitions with earthquake occurrences at short distances, we follow the approach by Cavers and Vasudevan (2015) to modify the weights w_{ij} in the weighted digraph by considering recurrences. Each earthquake (event) in a zone may have several recurring events in the record-breaking sense (Davidsen, 2008). For example, an event j is treated as a record with respect to an earthquake i if no event takes place within the spatial distance, d_{ij} , between i and j around i during the time interval $[t_i, t_j]$ with $t_i < t_j$. The next record-

breaking event, k , in the catalogue with reference to the original event, i , during the
 2 time interval $[t_i, t_k]$ with $t_i < t_k$ will have a spatial distance, d_{ik} , less than d_{ij} . The
 recurring events for one event in a given zone may fall into other zones or may be
 4 in the same zone. This flexibility adds to the possibility of interactions among
 zones. We first form the network of recurrences as described by Davidsen et al.
 6 (2008). The weight applied to each arc in the network of recurrences is derived
 empirically by using a total count of record breaking events between the
 8 corresponding earthquake zones and the distance involved (Cavers and Vasudevan,
 2015; Vasudevan and Cavers, 2013). Each recurrence from an earthquake a to an
 10 earthquake b in the sequence is given a weight between 0 and 1, with a weight equal
 to 1 if the distance between a and b is less than 50 km. If the distance is r with $r >$
 12 50 km and earthquakes a and b occur in Zones j and k respectively, a weight of

$$[L_{jk}(20000) - L_{jk}(r)] / [L_{jk}(20000) - L_{jk}(50)] \quad (3)$$

14 is given, where $L_{jk}(r)$ defined by Cavers and Vasudevan (2015) is the number of
 record-breaking events from zone j to zone k at distance at most r in the network of
 16 recurrences. The function in Equation (3) is a decreasing function in r giving a
 weight close to 0 when the distance r is large. Note that for $r = 50$ km, an output of
 18 1 is given while for $r = 20,000$ km, an output of 0 is given. As described by Cavers
 and Vasudevan (2015), a Markov chain with the inclusion of spatio-temporal
 20 complexity of recurring events is derived by summing the weights of the recurrence
 arcs corresponding to occurrences from state i to state j in consecutive time-
 22 intervals. Here, we calculated the time-series of the resulting state-to-state sequence
 (Figure 2a) and the corresponding transition frequency matrix (Figure 2b). There is
 24 one comment in order here. Figures 2a and 2b provide different representations of
 the same Markov chain. The first can be considered “dynamic”, because it shows

the time evolution of the transition from one state to another in consecutive time intervals of 9 days each. The second can be considered “static” because it shows the transition probabilities from one state to another but considering the whole earthquake sequence occurred during the whole observation period. However, they are not equivalent. We can go from the time-series data to transition-frequency matrix. We cannot go from the transition-frequency matrix to time-series without the additional information such as the catalogue and the record-breaking statistics of recurrences. Since it is obtained from the non-linear, non-stationary global earthquake sequence, we consider it non-linear and non-stationary as well, and hence, can be subjected to analysis methods. Although it is not shown here, the approach equally applies to earthquake catalogues from localized seismogenic zones.

3 Analysis methods and results

Each sample in the time-series shown in Figure 2a represents a “zone-configuration” state (Table 2). By definition, a zone-configuration has no zone or some zones or all zones highlighted by an earthquake or more in the optimally chosen time-interval. Going from one sample to the next does not only represent going from one state to the next but also shows the amplitude fluctuation between them. The adjacent states could represent the same zone-configuration or different zone-configurations. The time-series deduced from using the present approach with the five-zones marks the state-to-state fluctuations arising out of the fluctuations of oscillations or earthquake occurrences in the five-zones. We present in the following two analysis methods to glean an insight into the characteristics of the time-series.

3.1. Ensemble empirical mode decomposition as applied to state-to-state transition frequency sequence

For non-linear and non-stationary time-series, the method of empirical mode decomposition (EMD) has been recently proposed as an adaptive time-frequency analysis method (Huang et al., 1998, 1999) to decompose the original data into a basis set of intrinsic mode functions. Since the process that leads to the state-to-state transition frequency sequence or time-series is inherently non-linear and non-stationary, it is appropriate to apply the EMD to this data to understand the behavior of the intrinsic mode functions. The time-series (Figure 2a) reveals the fluctuations in the state-to-state transition frequencies arising out of varying occupancy of the zones from one time interval to the next. A situation would easily arise when two or three successive state-to-state transitions do not have earthquake occurrences in any of the zones studied. This would translate into intermittency in the time-series. Recent studies (Flandrin et al., 2004, 2005; Gledhill, 2003; Wu and Huang, 2004, 2009) support the idea of carrying out noise-added analyses with the EMD. The noise added analyses involves multiple realization of added noises to the time-series in question, leading to the ensemble EMD (EEMD), as proposed by Wu and Huang (2004, 2009).

In the EEMD, the signal or the time-series in question with the added Gaussian white noise, denoted as one trial, would populate the whole time-frequency space uniformly with the constituting component of different scales. Since the noise added in each trial is different, the ensemble mean of the noise cancels out and, hence, the signal resides in the intrinsic mode functions generated from the EEMD (Wu and Huang, 2009).

The time-series of state-to-state transition frequencies of the modified Markov chain model, $x_{sstf}(t)$, is taken as the signal. In each realization of the experiment, white noise, $w(t)$, is added to the signal. One might interpret the added Gaussian white noise as the possible random noise that would be encountered in the measurement process or in certain restrictions applied to the calculation of edge weights in the modified Markov chain. So, for the i^{th} realization,

$$x_{sstf,i}(t) = x_{sstf}(t) + w_i(t). \quad (4)$$

For each realization, we decompose the data with the added Gaussian white noise into intrinsic mode functions (IMFs). We consider the ensemble means of the IMFs of the decompositions as the final result.

Wu and Huang (2009) recommended that the ensemble size should be kept large and the amplitude of the added noise should not be small. We set the ensemble number for the number of realizations in EEMD large such that the noise series cancel each other in the final mean of the corresponding IMFs. For the two parameters, we used an ensemble size of 1000 and added noise with an amplitude of 0.2 times the standard deviation of the original data. We assume that the IMFs resulting from the EEMD represent a substantial improvement over the IMFs of the original EMD in that it utilizes the full advantage of the statistical characteristics of white noise to perturb the signal in its true solution neighbourhood, and to cancel itself after serving its purpose (Wu and Huang, 2009). EEMD results are summarized in Figures 3a to 3t with intrinsic mode functions followed by their state-to-state relative weight matrices derived from the basis set of the intrinsic mode functions of the time-series in a fashion identical to the original time-series. By summing the weights of the recurrence arcs corresponding to occurrences from state i to state j in consecutive time-intervals, we calculate the weighted matrix for state-

to-state transitions for each intrinsic mode function. Since the intrinsic mode
2 functions are the mathematical basis set of the original time-series, their static
displays or the weighted matrices show negative values. Identical to the sum of the
4 intrinsic mode functions yielding the original time-series, the sum of the weighted
matrices yields its transition frequency matrix. Similar to what Huang et al. (1998,
6 Figure 6 in their paper) have observed with the wind data, all of the intrinsic mode
functions excluding the trend for the wind data contain both positive and negative
8 values. We observe the same thing with the time-series in that the transition
probability values for the IMFs show both positive and negative values except that
10 the first two IMFs have negative values larger than the lowest positive value of the
trend. So, it is not surprising that the transition frequency matrices of the IMFs
12 contain the positive and negative numbers. However, viewing each IMF with the
trend starting with the third IMF will obviate this difficulty in that the high or low
14 frequency fluctuations ride on the trend with no negative values and the
corresponding transition-frequency matrices are positive. A similar observation has
16 been made by Huang et al. (1998, Figure 7) with their wind data. The observation
made with the first two IMFs suggests a limit on the proposed method, and it would
18 require further investigation.

The decomposition of the original time series into intrinsic mode functions and
20 the trend is dyadic in nature, as shown in Figure 3. This means that as we go from
the first intrinsic mode function to the second and so on, the interval increases by a
22 factor of 2 from $\Delta t = 9$ days to $\Delta t = 18$ days and so on. With an increase in the time
interval from one IMF to the next, we observe the relative weights of the state-to-
24 state transitions to vary. We also find that the state-to-state transitions within each
IMF occur in packets, and the number of packets progressively decreases. The last

packet of state-to-state transitions is persistent over the first 8 IMFs corresponding
2 to a time-interval of 9 days to 1152 days suggests the importance of the zone 4
earthquakes in understanding the earthquake sequencing. Although zone 4
4 earthquakes persist in the state-to-state transitions in the first few intrinsic mode
functions, the participation of other zones in state-to-state transitions becomes
6 significant in the higher intrinsic mode functions, IMFs 6 to 9.

In general, the intrinsic mode functions are characterized by (1) a certain number of
8 a pattern of rise and fall of the arc weights and (2) by a systematic decrease in the
frequency of the number of such patterns as one goes intrinsic mode function 1 to
10 the intrinsic mode function 9. Since the rise and fall of the arc weights covers the
entire catalogue of data, the periodicity that we notice could be intrinsic to
12 earthquake processes.

The Hilbert-Huang amplitude spectrum of the time series, shown in Figure 4,
14 reveals at least two important features: (1) The temporal fluctuations in amplitudes
occur in packets, each packet containing a set of zone to zone interactions. The
16 oscillatory behaviour of packets contains certain periodicity within the earthquake
sequence. A periodic trend at low frequencies suggests the role of zone 4 (Trenches)
18 and zone 0 (Intraplate). A higher power at 2004/03/06 and 2005/05/30 indicates the
importance of zone 4 with earthquakes of larger magnitude prompting a cascade of
20 aftershocks in zone 4 and main shocks in zones that are in close proximity to zone
4. (2) The frequency-dependence of amplitude packets encapsulates the relative
22 importance of the interaction among multiple zones over different time intervals.

We interpret them to mean that certain state-to-state transitions involving zone 4 are
24 important over a range of frequencies.

3.2 Evaluation of fractality in a state-to-state transition frequency sequence

Earthquake occurrences have been modelled to be stochastic point processes
 2 (Thurner et al., 1997; Telesca et al., 2001, 2005, 2009 and 2011; Flores-Marquez
 and Valverde-Esparza, 2012). One representation of the point process is to examine
 4 the inter-event time-intervals. The resulting inter-event interval probability density
 function says something about the behavior of the times between events. We do not
 6 know anything about the information contained in the relationships among these
 items. Since successive events do not occur in constant time-intervals, another
 8 representation of a point process is given by dividing the time-axis into equally
 spaced contiguous counting windows of duration τ , and producing a sequence of
 10 counts that fall within each time-window. For example, for the k^{th} time-window,
 the expression for the number of counts, $N_k(\tau)$, is given by

$$12 \quad N_k(\tau) = \int_{t_{k-1}}^{t_k} \sum_{j=1}^n \delta(t - t_j) dt \quad (5)$$

where $N_k(\tau)$ is the number of earthquakes in the k^{th} window (Figure 5; panels a to
 14 d). The correlation in the process $\{N_k(\tau)\}$ is the correlation in the underlying point
 process (Lowen and Teich, 1993a, 1993b; Thurner et al., 1997; Telesca et al., 2001,
 16 2005, 2009, 2011) have accessed such a representation of the point-processes to
 underscore the existence or non-existence of fractality in them. They have two
 18 calculable measures, Fano factor (FF) and Allan factor (AF), to quantify the
 fractality of the process (Lowen and Teich, 1993a, 1993b; Thurner et al., 1997;
 20 Telesca et al., 2001, 2005, 2009, 2011; Flores-Marquez and Valverde-Esparza,
 2012).

22 The Fano factor is a measure of correlation over different timescales (Thurner et
 al. 1997). It is defined as the ratio of the variance of the number of events in a
 24 specified counting time τ to the mean number of events in the counting time, as is
 given by

$$FF(\tau) = \frac{\langle N_k^2(\tau) - N_k(\tau) \rangle^2}{\langle N_k(\tau) \rangle} \quad (6)$$

2

where $\langle \rangle$ denotes the expectation value. Lowen and Teich (1995) point out that
 4 the FF of a fractal point process follows a power law with the power-law exponent,
 α , obeying $0 < \alpha < 1$. In other words, the FF is always greater than 1. For Poisson
 6 processes, the FF is always near unity for all counting times, and the fractal
 exponent is approximately equal to zero.

8

The Allan factor is a relation with the variability of successive counts (Allan,
 1996; Barnes and Allan, 1966). It is the ratio of the variance of successive counts
 10 for a specified counting time τ divided by twice the mean number of events in the
 counting time. The expression of AF is given as

$$AF(\tau) = \frac{\langle N_{k+1}(\tau) - N_k(\tau) \rangle^2}{2\langle N_k(\tau) \rangle} \quad (7)$$

12

Similar to the FF , the AF assumes values near unity for Poisson processes. Telesca
 14 et al. (2009, 2011; henceforth, referred to as Telesca's approach) and Flores-
 Marquez and Valverde-Esparza (2012) have shown the power-law exponent for the
 16 AF to be $0 < \alpha < 1$.

In this paper, we examine both the results of Telesca's approach to the initial
 18 catalogue of the data used and of the new representation of the point process with a
 Markov chain model. For the working model, we compute the state-to-state
 20 transition frequencies as described by Nava et al. (2005) and as applied to global
 seismicity (Vasudevan and Cavers, 2012; Cavers and Vasudevan, 2013).
 22 Expressions similar to equations (6) and (7) can be derived if we know the optimal
 time-interval for the Markov chain model. Since we know the optimal time-interval,
 24 we introduce a sequence of state-to-state transition frequencies, $\{N_{sstf,k}(\tau)\}$, with

$N_{sstf,k}(\tau)$ referring to the weight of state-to-state transitions over the k^{th} window for the optimal time-interval, as is shown in Figure 5f. For an easy understanding of Figure 5f, we have included Figure 5e.

There are a few observations to be made. First, $N_{sstf,k}(\tau)$ is not necessarily an integer number for any k^{th} window. Following the definition of a state, in the context of a directed graph of a Markov chain model, a state-to-state transition refers to an edge of a graph. It is the weight associated with the edge of the directed graph that plays an important role. Since we have used a modified Markov chain model which includes the influence of the event recurrences in the record-breaking sense, the above expression includes their weights as well in the computation of $N_{sstf,k}(\tau)$. The sequence of state-to-state transition frequencies, $\{N_{sstf,k}(\tau)\}$, yields a time-series. This time-series is the new expression of the point-process where the weighted edges of directed graph of the modified Markov chain represent the significance of the earthquakes between states. This new alternative representation signifies the behavior of the state-to-state transition frequencies over a large time window. Here, seeking to find the time-correlative behavior of the time-series would be of great importance since this would give us an opportunity to see the interaction of zones considered in a collective sense.

Here, we seek to understand the correlative behavior by looking at the two statistical measures, FF_{sstf} and AF_{sstf} , as defined below:

$$FF_{sstf}(\tau) = \frac{\langle N_{sstf,k}^2(\tau) - N_{sstf,k}(\tau) \rangle^2}{\langle N_k(\tau) \rangle} \quad (8)$$

$$AF_{sstf}(\tau) = \frac{\langle N_{sstf,k+1}(\tau) - N_{sstf,k}(\tau) \rangle^2}{2\langle N_{sstf,k}(\tau) \rangle} \quad (9)$$

The behavior of the two measures, FF_{sstf} and AF_{sstf} , with respect to the optimal time-interval should shed some light on the correlative behavior of the time-series but

also on the selective clustering of the certain state-to-state transitions. We consider

2 this knowledge to be useful for forecasting purposes.

In our adaptation of the sum of edge weights for the state-to-state transition
4 frequencies as a new representation of a point-process embedded in the modified
Markov chain here, the arguments of Thurner et al. (1997) and Telesca et al. (2001,
6 2005, 2009, 2011) would apply. This means that the FF of the modified Markov
chain sequence would follow a power-law with the power-law exponent, α ,
8 satisfying $0 < \alpha < 1$.

Extending this to FF_{sstf} and AF_{sstf} , as is shown in Figure 6 (panels 6c and 6d), we
10 find that the power law exponent calculated, corresponding to the least-squares fit
of the data is greater than zero (0.27 and 0.30 respectively). They suggest not only
12 the fractality of the modified Markov chain sequence for optimal time-interval but
also the deviation from the Poissonian behavior of earthquake sequencing
14 considered in this present study.

16 **4 Discussion and conclusions**

Thurner et al. (1997) pointed out that the sequence of counts, generated by recording
18 the number of events in successive counting time-windows of certain length,
contained information about the point process depicted by the set of event times.
20 This idea was further tested in understanding the dynamics of earthquake
sequencing (Telesca et al., 2009, 2011; Flores-Marquez and Valverde-Esparza,
22 2013), and in particular, the fractal behavior of the sequence of counts. We know
that this idea was initially restricted to the sequence of counts for varying windows
24 of interval-times. However, for comparison purposes, we calculated the Fano factor
and the Alan factor for the initial catalogue of data using equations (6) and (7). We

include their graphs in Figure 6 (panels 6a and 6b). Similar to observations made
2 by Telesca et al. (2009) with the earthquake data from the Taiwan region, we find
the presence of two distinctly different regions of scaling behaviour. For small time-
4 intervals, we also observe the Poisson behaviour. Since very poor statistics at time-
scales larger than 10^8 seconds would influence the Fano factor and the Allan factor,
6 we have restricted our analysis to 3.17 years or roughly 10^8 seconds.

In our description of the directed graph of the Markov chain model of any
8 earthquake sequencing, regional or global, we stress the significance of the state-to-
state transition probabilities for multiple zones that span the sequence of
10 earthquakes over an optimal time window (Cavers and Vasudevan, 2013;
Vasudevan and Cavers, 2013). In other words, the edges of the directed graph carry
12 weights. We conjecture that these weights represent a new definition of the point
process. Furthermore, a consideration of the earthquake recurrences within each
14 zone and among zones, following the concept of recurrences in the record-breaking
sense (Davidsen et al., 2008), leads to an empirically-determined distance-
16 dependent weights for the edges. Unlike extending the idea of the sequence of
counts where every event occurrence augments the counting value by unity (Turner
18 et al., 1997; Telesca et al., 2009, 2011; Flores-Marquez and Valverde-Esparza,
2013), we consider the summing of the weights for each edge such that the sum
20 represents a “pulse” for each state-to-state transition. We analyse the resulting time-
series from the point of view of its Fano factor and Allan factor. There is evidence
22 for fractality of the multi-state modified Markov chain to represent the earthquake
sequencing, as is revealed by the power-law scaling behavior present in the Fano
24 and Allan factors with their respective exponents of 0.27 and 0.30 (Figure 6, panels

6c and 6d). However, it is important to note that the exponents of the power-laws

in both cases have a smaller value than those observed for the initial catalogue.

Cavers and Vasudevan (2013) interpreted the Markov chain of 32-states for five-
distinctly different zones to contain the basic combinatoric structure superimposed
by the thumb-print of the undulatory structure of the recurrence weights. Since the
earthquake sequencing is in general non-linear and non-stationary, we contend that
the time-series representing the above Markov chain is also non-linear and non-
stationary, and is conducive to an ensemble empirical mode decomposition (EEMD)
procedure to understand its intrinsic mode functions (IMFs). The ensemble
empirical model decomposition of the time-series leads to nine intrinsic mode
functions and a trend. Each one of the IMFs reveals the amplitude fluctuation of
the state-to-state transitions. While there is a commonality in the relative dominance
of the subduction-style earthquakes, represented by the top right corner grid of the
relative weight matrices (Figure 3), the presence or absence of certain state-to-state
transitions in certain IMFs reveals the importance of integral multiples of the
optimal time-interval.

A simple observation of the first 6 or 7 IMFs stresses the importance of multiple-
zone approach to global seismicity problem in that the earthquake sequencing for
the time period we considered has similar oscillatory behavior of the state-to-state
transition probabilities from the point of view of the amplitude scaling and the
oscillating period. The growth and decay of oscillations in easily identifiable
packets in each IMF following certain periodicity is an intrinsic signature of the role
of multiple zones in earthquake sequencing.

Acknowledgements. The authors would like to express deep gratitude to the department of mathematics and statistics for support and computing time. M.C. acknowledges the Natural Sciences and Engineering Research Council of Canada for a post-doctoral fellowship during the period of 2010 to 2012 when this research was first initiated. The authors express sincere thanks to Dr. Y.Y. Kagan for making the global seismicity data available on the net. They thank Dr. Reik Donner of Potsdam Institute for Climate Research, Potsdam and an anonymous referee for constructive criticisms of the manuscript and helpful suggestions to improve the original version of the manuscript.

References

- Allan, D. W.: Statistics of atomic frequency standards, Proc. IEEE, 54, 221-230, 1966.
- Barnes, J. A., and Allan, D. W.: A statistical model of flicker noise, Proc. IEEE, 54, 176-178, 1966.
- Bird, P.: An updated digital model of plate boundaries, Geochem. Geophys. Geosys., 4(3), 1027, doi:10.1029/2001GC000252, 2003.
- Bohnenstiehl, D.R., Tolstoy, M., Smith, D.K., Fox, C.G., and Dziak, R.P.: Time-clustering behavior of spreading-center seismicity between 15 and 35°N on the Mid-Atlantic Ridge: observations from hydroacoustic monitoring, Phys. Earth and Planet. Interiors, 138, 147-161, 2001.
- Cavers, M., and Vasudevan, K.: An application of Markov Chains in seismology, The Bulletin of the Int. Linear Algebra Soc., 51, 2-7, 2013.
- Cavers, M., and Vasudevan, K.: Spatio-temporal Markov Chain (SCMC) model using directed graphs: Earthquake sequencing, Pure and Applied Geoph., 172, 225-241, 2015, DOI 10.1007/s00024-014-0850-7.
- Çınlar E.: Introduction to Stochastic Processes. Englewood Cliffs, NJ, USA: Prentice Hall, 106-277, 1975.
- Davidson, J., and Schuster, H.G.: Simple model for $1/f^\alpha$ noise, Phys. Rev. E, 65, 026120, 2002.

- 2 Davidsen, J., Grassberger, P., and Paczuski, M.: Networks of recurrent events, a
theory of records, and an application to finding causal signatures in seismicity,
4 Phys. Rev. E, 77, 66-104, 2008.
- 6 DeMets, C., Gordon, R.G., Argus, D.F., and Stein, S., Current plate motions,
Geophys. J. Int., 101(2), 425-478, 1990.
- 8 DeMets, C., Gordon, R.G., and Argus, D.F., Geologically current plate motions,
10 Geophys. J. Int., 181, 1-80, 2010.
- 12 Flandrin, P., Rilling, G., and Gonçalves, P.: Empirical mode decomposition as a
filterbank, IEEE Signal Process. Lett., 11, 112–114, 2004.
- 14 Flandrin, P., P. Gonçalves and G. Rilling, 2005: EMD Equivalent Filter Banks,
16 from Interpretation to Applications. In *Hilbert-Huang Transform : Introduction
and Applications*, pp 67-87, Ed. N. E. Huang and S. S. P. Shen, World
18 Scientific, Singapore, 360pp
- 20 Flores-Marquez, E.L., and Valverde-Esparza, S. M.: Non-Linear Analysis of Point
Processes Seismic Sequences in Guerrero, Mexico: Characterization of
22 Earthquakes and Fractal Properties, Earthquake Research –
Seismology, Seismotectonic and Earthquake Geology, Dr. Sebastiano D'Amico
24 (Ed.), 2012., ISBN: 978-953-307-991-2, InTech, DOI: 10.5772/29173.
- 26 Gledhill, R. J.: Methods for Investigating Conformational Change in
Biomolecular Simulations. A dissertation for the degree of Doctor of
28 Philosophy at Department of Chemistry, the University of Southampton, 201pp,
2003.
- 30 Herrera, C., Nava, F. A. and Lomnitz. C.: Time-dependent earthquake hazard
32 evaluation in seismogenic systems using mixed Markov Chains: An application
to the Japan area, Earth Planets Space, 58, 973-979, 2006.
- 34 Huang, N. E., Shen, Z., Long, S. R., Wu, M. C., Shih, E. H., Zheng, Q., Yen, N.-
36 C., Tung, C. C. and Liu, H. H.: The empirical mode decomposition method and
the Hilbert spectrum for non-stationary time series analysis, Proc. R. Soc.
38 (London) A, 454, 903–995, 1998.
- 40 Huang, N. E., Shen, Z., and Long, S.R.: A new view of nonlinear water waves:
The Hilbert spectrum, Ann. Rev. Fluid Mech., 31, 417-457, 1999.
- 42 Jarvis, J.P. and Shier, D. R.: Graph-theoretic analysis of finite Markov chains, in:
44 *Applied Mathematical Modeling: A Multidisciplinary Approach*, edited by D.
R. Shier and K. T. Wallenius, CRC Press, 1996.
- 46 Kagan, Y.Y., and Jackson, D. D.: Long-term earthquake clustering, Geophys. J.
48 Int., 104, 117-133, 1991.
- 50 Kagan, Y.Y., Bird, P., and Jackson, D.D.: Earthquake patterns in diverse tectonic

- zones of the globe, *Pure Appl. Geophys.*, 167, 721-741, 2010.
- 2 Kanamori, H.: Earthquake prediction: An overview, in *International Handbook of*
4 *Earthquake & Engineering Seismology*, edited by W. H. K. lee, H. Kanamori,
P.C. Jennings, and C. Kisslinger, pp. 1205-1216, Academic Press, Amsterdam,
6 2003.
- 8 Lowen, S.B., and Teich, M. C.: Fractal renewal processes generate 1/f noise, *Phys.*
Rev. E., 47(2), 992-1001, 1993.
- 10 Lowen, S. B. and Teich, M. C.: Estimation and Simulation of Fractal Stochastic
12 Point Processes, *Fractals*, 3, 183–210, 1995.
- 14 Nava, F. A., Herrera, C., Frez, J., and Glowacka, E.: Seismic hazard evaluation
using Markov chains: Application to the Japan area, *Pure Appl. Geophys.*, 162,
16 1347-1366, 2005.
- 18 Serinaldi, F., and Kilsby, C.G.: On the sampling distribution of Allan factor
estimator for a homogeneous Poisson process and its use to test
20 inhomogeneities at multiple scales, *Physica A: Statistical Mechanics and its*
Applications, 392(5), 1080-1089, 2013.
- 22 Telesca, L., Cupmo, V., Lapenna, V., and Macchiato, M.: Statistical analysis
24 of fractal properties of point processes modeling seismic sequences, *Phys. Earth*
Planet Int., 125, 65-83 (2001).
- 26 Telesca, L., and Lovallo, M.: Investigating non-uniform scaling behaviour in
28 temporal fluctuations of seismicity, *Nat. Hazards Earth Syst. Sci.*, 8, 973-876,
2008.
- 30 Telesca, L., Chen, C.-C., and Lee, Y.-T.: Scaling behaviour in temporal
32 fluctuations of crustal seismicity in Taiwan, *Nat. Hazards Earth Syst. Sci.*, 9,
2067-2071, 2009.
- 34 Telesca, L., Cherkaoui, T.-E., and Rouai, M.: Revealing Scaling and Cycles
36 in Earthquake Sequences, *Int. J. Nonlinear Sci.*, 11(2), 137-142, 2011.
- 38 Turner, S., Lowen, S.B., Feurstein, M.C., Heneghan, C., Feichtinger, H.G., and
Teich, M.C.: Analysis, synthesis, and estimation of fractal-rate stochastic
40 point processes. *Fractals*, 5, 565-596, 1997.
- 42 Ünal, S. and Çelebioğlu, S.: A Markov chain modeling of the earthquakes
occurring in Turkey, *Gazi University Journal of Science*, 24(2), 263-274
44 (2011).
- 46 Ünal S., Çelebioğlu S., and Özmen, B.: Seismic hazard assessment of Turkey by
statistical approaches, *Turkish J. Earth Sci.*, 23, 350-360, 2014.
- 48 Vasudevan, K., and Cavers, M.: A graph theoretic approach to global earthquake
50 sequencing: A Markov chain model, Presented at the American Geophysical

- 2 Union's Fall Meeting, San Francisco, California, December 3-7, 2012, Poster
ID: NG13A-1515, 2012.
- 4 Vasudevan, K., and Cavers, M.: Insight into earthquake sequencing: Analysis and
interpretation of time-series of the Markov chain model., Presented at the
6 American Geophysical Union's Fall Meeting, San Francisco, California,
December 9-13, 2013, Poster ID: NG24A-06-1574, 2013.
- 8 Wu, Z., and Huang, N.E.: A study of the characteristics of white noise using the
empirical mode decomposition method, Proc. R. Soc. (London) A., 460, 1597-
10 1611, 2004.
- 12 Wu, Z., and Huang, N. E.: Ensemble empirical mode decomposition: A noise-
assisted data analysis method, Adv. Adapt. Data Anal., 1(1), 1-42, 2009.

List of tables

2

Table 1. Tectonic zone identifier, tectonic zone and the number of earthquakes considered for M_w
4 > 5.6 and depth < 70 km from 1982/01/01 to 2007/03/31.

6

Table 2. Zone and state definition used in the construction of a directed graph of a Markov chain.
‘0’ and ‘1’ refer to the no occurrence or occurrence of an earthquake for a given zone. For five

8

zones, there are 32 states.

Table 1.

Zone identifier	Tectonic zone	N	N/N_{total}
0	Plate-interior	237	0.0351
1	Active continent	898	0.1330
2	Slow-spreading ridges	487	0.0721
3	Fast-spreading ridges	723	0.1071
4	Trenches	4407	0.6527
	Global (or N _{total})	6752	1.0000

2

Table 2.

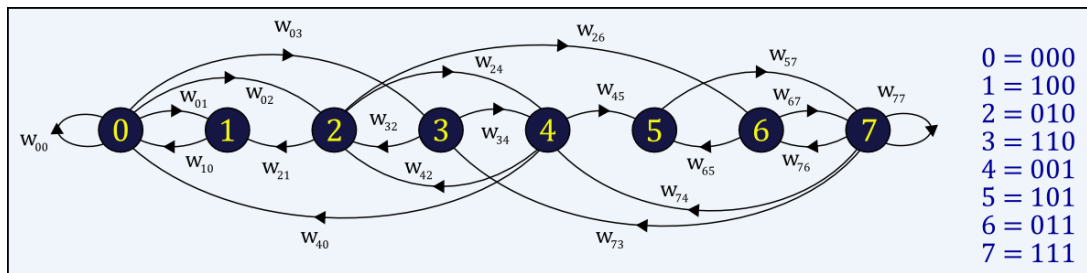
State	Zone 4	Zone 3	Zone 2	Zone 1	Zone 0
0	0	0	0	0	0
1	0	0	0	0	1
2	0	0	0	1	0
3	0	0	0	1	1
4	0	0	1	0	0
5	0	0	1	0	1
6	0	0	1	1	0
7	0	0	1	1	1
8	0	1	0	0	0
9	0	1	0	0	1
10	0	1	0	1	0
11	0	1	0	1	1
12	0	1	1	0	0
13	0	1	1	0	1
14	0	1	1	1	0
15	0	1	1	1	1
16	1	0	0	0	0
17	1	0	0	0	1
18	1	0	0	1	0
19	1	0	0	1	1
20	1	0	1	0	0
21	1	0	1	0	1
22	1	0	1	1	0
23	1	0	1	1	1
24	1	1	0	0	0
25	1	1	0	0	1
26	1	1	0	1	0
27	1	1	0	1	1
28	1	1	1	0	0
29	1	1	1	0	1
30	1	1	1	1	0
31	1	1	1	1	1

List of figures

- Fig 1.** A graph representation of earthquake sequencing with arcs (with weights w_{ij}) representing transitions between states.
- Fig 2.** (a) A time-series of the state-to-state transition frequencies of the modified Markov chain model of the earthquake sequencing. The sampling time (Δt) of 9 days is used. (b) The state-to-state transition frequencies of the modified Markov chain model of the earthquake sequencing.
- Fig 3.** Ensemble empirical mode decomposition of the time series. (a-i) Intrinsic mode functions from the first to the ninth; (j) Intrinsic mode function of the trend; (k-s) State-to-state relative weight matrices for the intrinsic mode functions from the first to the ninth; (t) State-to-state relative weight matrix of the trend. Time steps and the corresponding calendar dates: 0 $\Delta t \rightarrow$ 1982/01/01; 200 $\Delta t \rightarrow$ 1986/12/06; 400 $\Delta t \rightarrow$ 1991/11/10; 600 $\Delta t \rightarrow$ 1996/10/14; 800 $\Delta t \rightarrow$ 2001/09/18; 1000 $\Delta t \rightarrow$ 2006/08/23; 1024 $\Delta t \rightarrow$ 2007/03/27. We provide this information here to avoid any cluttering of the plots.
- Fig 4.** Hilbert-Huang amplitude spectrum of the intrinsic functions.
- Fig 5.** Representation of a point process (panels a to d) versus representation of a state-to-state transition (panels e and f). (Adapted from Thurner et al. (1997))
- Fig 6.** (a) and (b) show the Fano and Allan factor graphs, respectively, derived from the earthquake catalogue data using the approach of Telesca et al. (2001, 2008, 2009, 2011); (c) and (d) show the Fano and Allan factor graphs, respectively, for the time series of the state-to-state transition frequencies of the modified Markov chain model of the earthquake sequencing.

Figure 1.

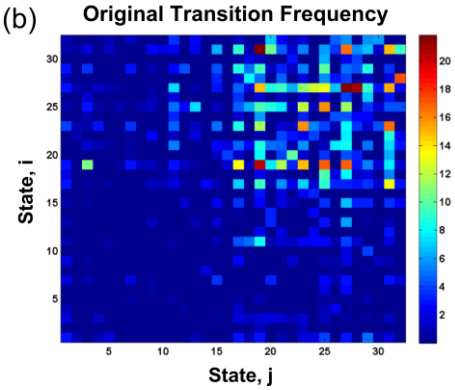
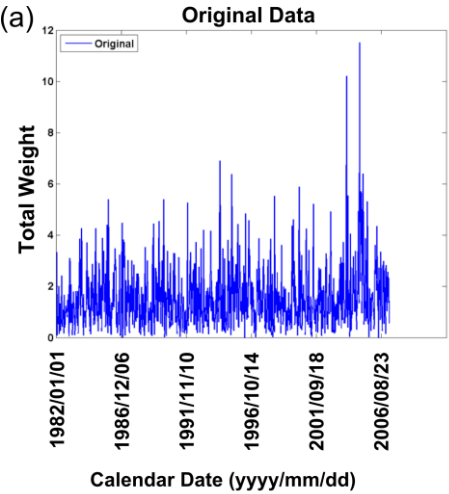
2



4

Figure 2.

2



4

Figure 3.

2

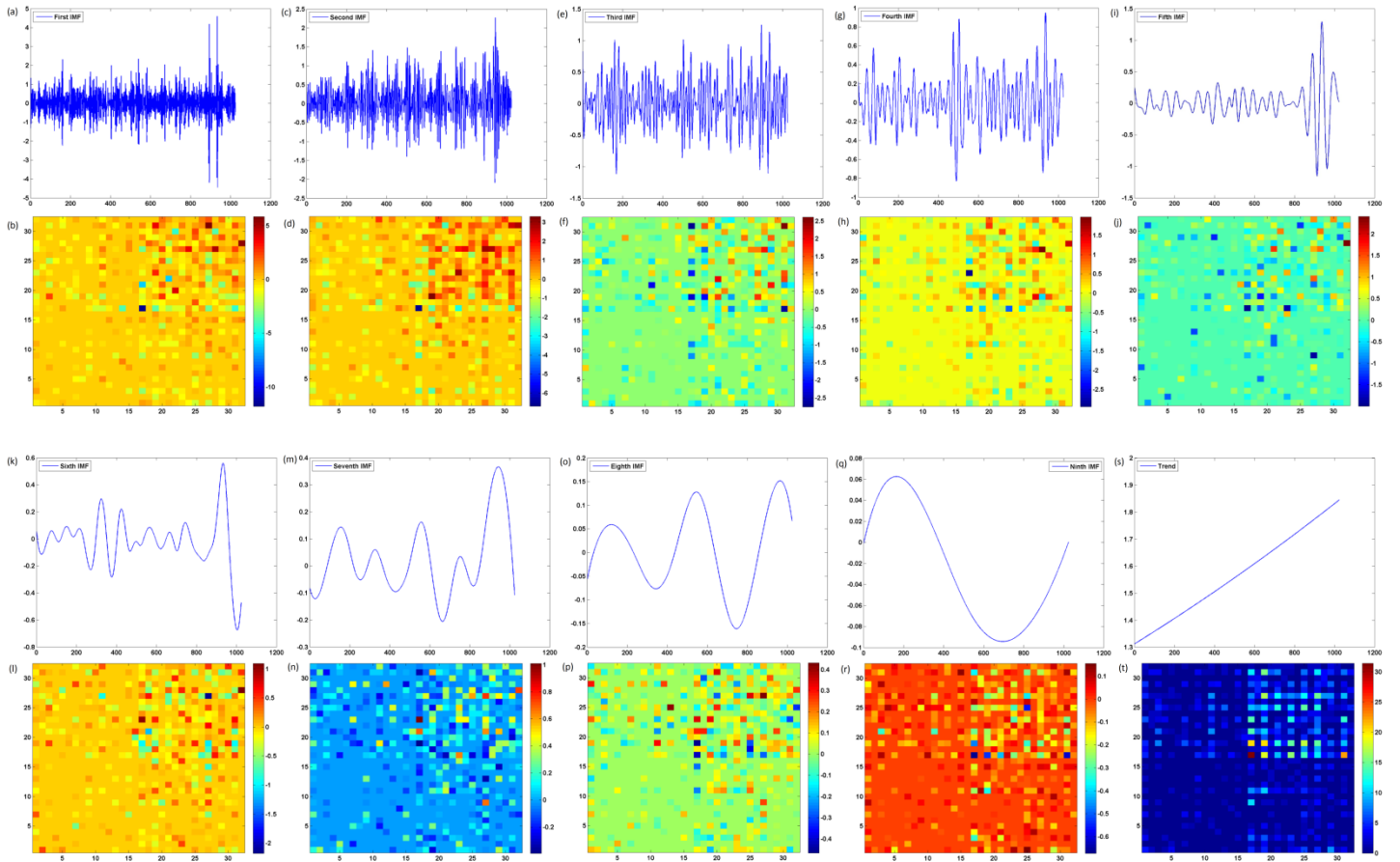
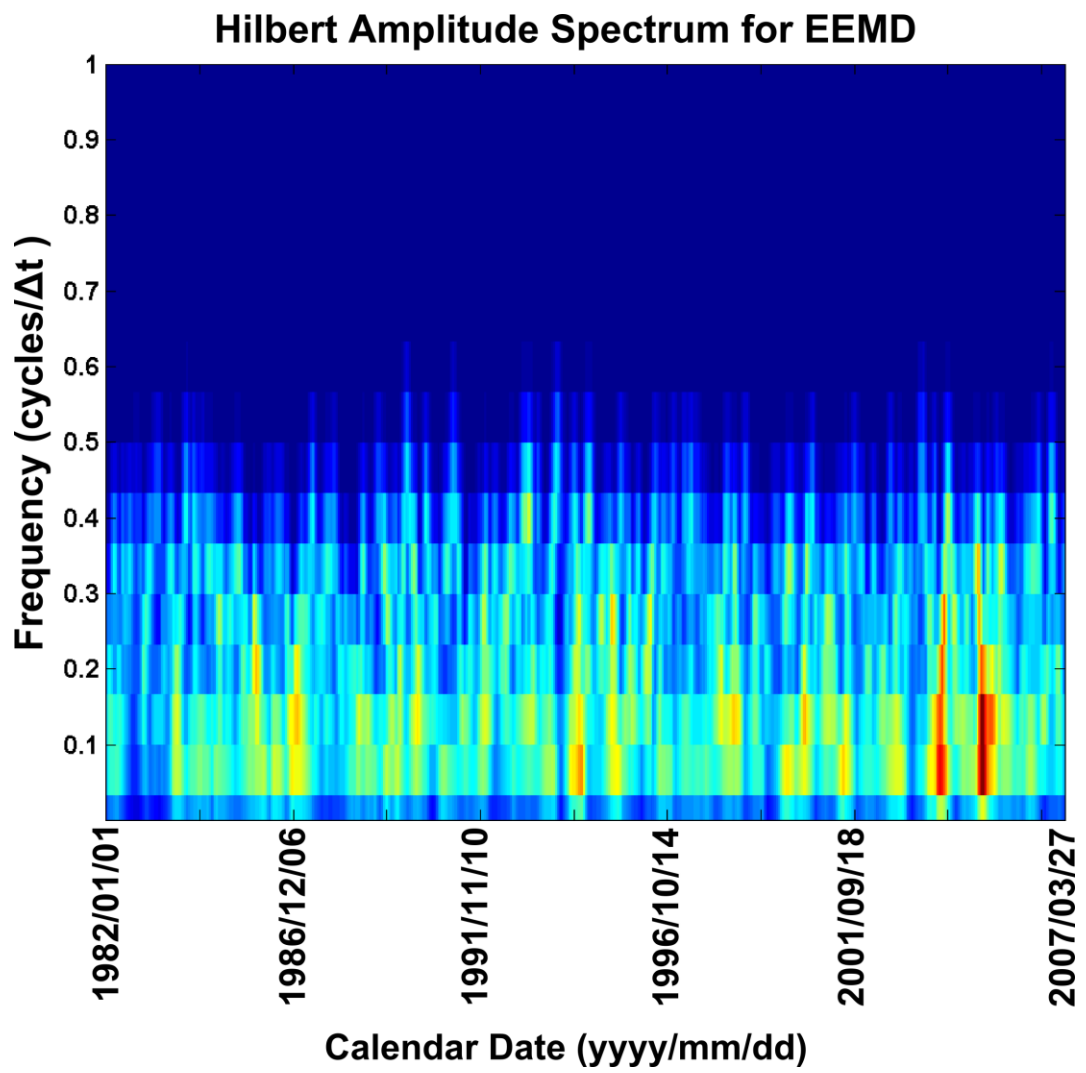


Figure 4.

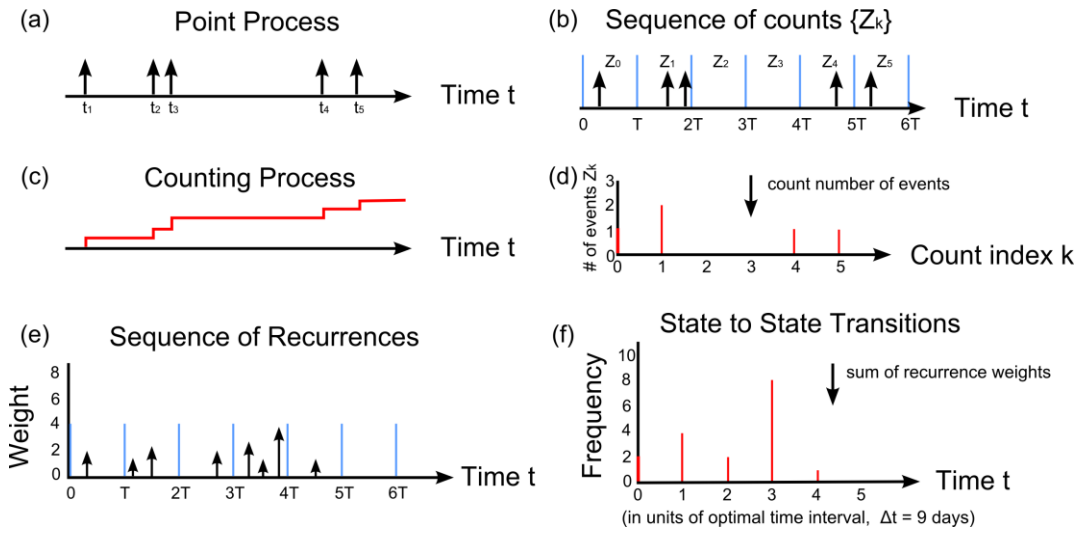
2



4

Figure 5.

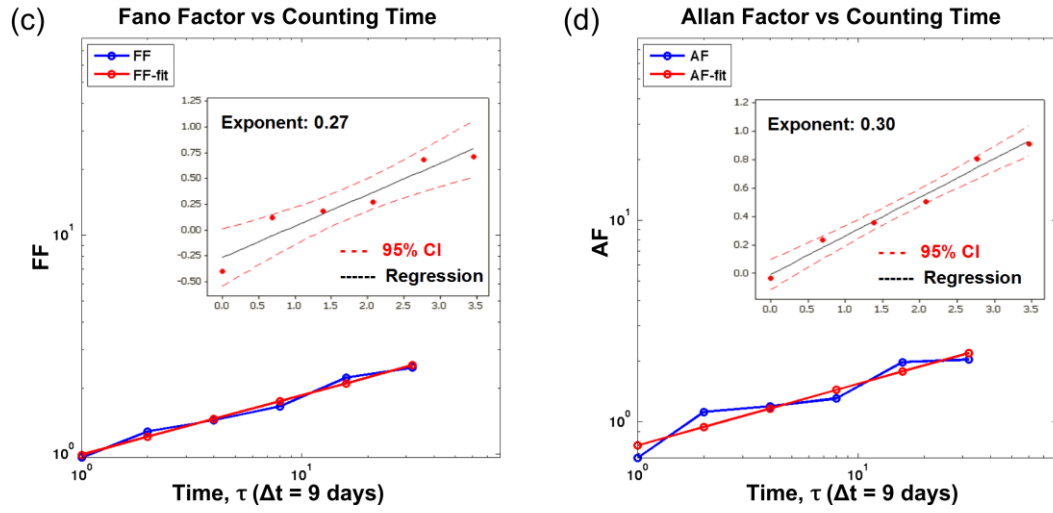
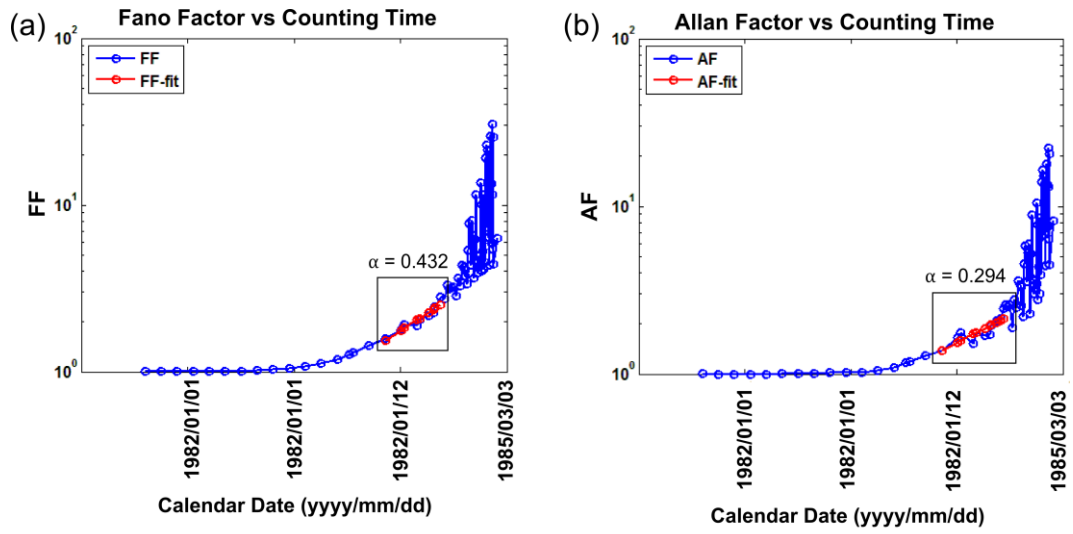
2



4

Figure 6.

2



4